Effect of Mesophase Order on the Dynamics of Side Group Liquid Crystalline Polymers

Maria L. Auad,[†] Michael D. Kempe,[†] Julia A. Kornfield,[†] Stanley Rendon,[‡] Wesley R. Burghardt,*[,‡] and Kyunghwan Yoon[§]

Department of Chemistry and Chemical Engineering, California Institute of Technology, Pasadena, California 91125, Department of Chemical and Biological Engineering, Northwestern University, Evanston, Illinois 60208, and Department of Mechanical Engineering, Dankook University, Seoul, Korea

Received March 15, 2005; Revised Manuscript Received June 8, 2005

ABSTRACT: Rheology and X-ray scattering were employed to probe the viscoelastic properties and structural transitions of model cyano-biphenyl-based side-group liquid−crystalline polymers (SGLCPs) with molecular weights ranging from 91 to 1900 kg/mol. Temperature-dependent rheological data show a rapid change in dynamics over a small temperature range. Small-angle X-ray scattering reveals these changes to be associated with an isotropic to smectic transition with an appreciable biphasic region. The presence of a biphasic region is attributed to inhomogeneity in chain structure resulting from incomplete attachment of mesogens to every monomeric unit in the SGLCP polymer. While isotropic and smectic phase data may be separately time−temperature shifted to create master curves for the individual phases, we argue against attempts to achieve superposition between the two phases in the high-frequency regime, since smectic ordering may not simply slow the dynamics but also increase the modulus of the sample. Molecular weight has a strong influence on rheology in the isotropic phase, where an entanglement plateau emerges; however, the smectic-phase rheology is dominated by the layer structure and is fairly insensitive to molecular weight.

1. Introduction

Side-group liquid−crystalline polymers (SGLCPs) consist of stiff mesogenic units laterally attached to a flexible polymeric backbone via short, flexible spacers. The partial coupling between the mesogens and the backbone leads to distinctive macroscopic relationships between strain and orientation that may find application in technologies such as stress and photomechanical sensors and actuators.[1−5] To realize these applications, it is vital to gain a comprehensive understanding of the SGLCP rheology as well as the effect that the flow history has on molecular alignment. It has been found that the coupled dynamics of the backbone and mesogens give rise to intriguing rheological consequences in the liquid crystalline state.

Early SGLCP melt rheology investigations concluded that the flexible backbone dominates the dynamics in nematic SGLCPs, overwhelming typical liquid-crystalline characteristics.[6−8] These results are surprising, given that the liquid-crystalline order of small-molecule LCs, lyotropic rodlike LCPs, and thermotropic main-chain LCPs has a profound effect on their rheology.[9−12]

Investigations of the viscoelasticity of SGLCPs using steady shear have shown that isotropic-to-nematic phase transitions have no effect on the melt viscosity.[8] Contrary to these results, Rubin et al.[13] determined that nematic order produces significant changes in the dynamics of entangled SGLCP systems when compared to the isotropic phase. The rheology of nematic SGLCPs has continued to attract interest.[14−17]

Fewer efforts, however, have examined the viscoelasticity and phase behavior of *smectic* SGLCPs.[6,13,19,20] The positional order in smectic LCs leads to more pronounced rheological consequences upon order than is seen in nematic LCs. Colby et al. reported that smectic SGLCPs exhibit a broad relaxation time distribution without an accessible terminal regime and document dramatic changes in dynamics upon transition from the nematic to smectic phase.[6] Rubin et al. observed similar changes in dynamics upon a nematic to smectic transition in their study.[13] Wewerka et al. employed linear rheology to probe the viscoelastic properties and structural transitions in model norbornene-based SGLCPs.[19] In their study, SGLCPs with long spacer groups were found to exhibit smectic ordering at lower temperatures, in which the characteristic layered morphology dominates the storage modulus.[19] More recently, Kim and Han have compared nematic and smectic SGLCPs and report much more dramatic changes in linear viscoelasticity for an isotropic−smectic transition than for a isotropic−nematic transition.[20]

In this investigation, we report on the synthesis, phase behavior, and viscoelasticity of a series of smectic SGLCPs of varying molecular weight. The structural and rheological properties of these liquid crystalline materials were investigated using combined rheology and X-ray techniques to identify and classify the nature of the mesophase transitions. (A separate paper describes flow-induced alignment of the smectic layers.[21]) We find that the interplay between molecular weight, polydispersity, and degree of mesogen attachment explains the origin and width of a smectic−isotropic biphase.

* To whom correspondence should be addressed. E-mail: w-burghardt@northwestern.edu.
[†] Department of Chemistry and Chemical Engineering, California Institute of Technology, Pasadena, California 91125.
[‡] Department of Chemical and Biological Engineering, Northwestern University, Evanston, Illinois 60208.
[§] Department of Mechanical Engineering, Dankook University, Seoul, Korea.

10.1021/ma050551f CCC: $30.25
Published on Web 07/16/2005

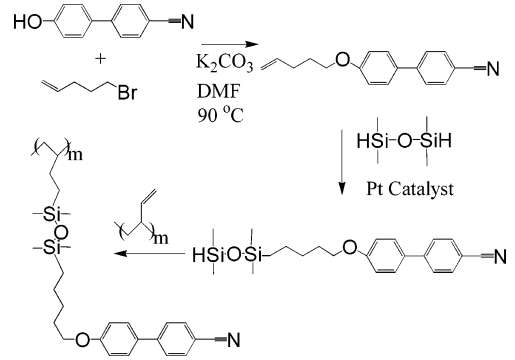

Figure 1. Method for synthesis of SGLCP with a siloxane spacer. For our system $m = 200-2800$. The product polymer is named PBSiCB5 since it was made with a 1,2-polybutadiene parent polymer, using a siloxane linking group, a cyanobiphenyl mesogenic unit, and a pentyl group in the spacer.

2. Experimental Section

2.1. Polymer Synthesis. The polymers used in this study were synthesized by mesogen attachment to pendant vinyl groups of an anionically synthesized[22−24] 1,2-polybutadiene backbone (Figure 1). This technique was used so that large molecular weight polymers could be obtained while still maintaining relatively low polydispersity. The techniques used to attach the mesogenic group are similar to those used by other researchers;[25−28] however, due to the large molecular weight of our polymers, additional effort was required for reactant and product purification.

The 4′-cyano-4-hydroxylbiphenyl was obtained from TCI America and purified on a silica gel column using a mixture of 33% ethyl acetate in hexane. All other chemicals were purchased from Aldrich and were used without further purification. The spacer was attached using the Williamson ether synthesis technique with 30% excess 5-bromopentene in DMF with 1 equiv of anhydrous potassium carbonate at a temperature of 90 °C for 3 h, Figure 1. The product 4-cyano-4′-(4-penteneoxy)-biphenyl, CBV5, was precipitated out by the addition of water and purified on a silica gel column using 50% dichloromethane in hexane with an overall yield of ∼95%.

A 10× excess of tetramethyldisiloxane (TMDS) dissolved in anhydrous toluene was used in the next step to reduce the amount of dimer formed. It was attached to the CBV5 in an anhydrous toluene solution using a few drops of the catalyst PC085, platinum-cyclovinyl-methylsiloxane complex, or PC072, platinum-divinyltetramethyldisiloxane complex in xylene, both of which were purchased from United Chemical Technology. This reaction, producing 4-cyano-4′-(5-(1,1,3,3-tetramethyldisiloxane)pentoxy) biphenyl (CBSi5), ran overnight at room temperature and was monitored using thin-layer chromatography.

Since only a small amount of disilane byproducts are necessary to cross link a large molecular weight polymer, the CBSi5 must be highly purified prior to attachment to the 1,2-polybutadiene backbone. The excess TMDS, boiling point (bp) 71 °C, was removed by boiling under vacuum at 50 °C. Since TMDS is more volatile than the toluene solvent, bp 110 °C, the product should be completely free of TMDS. Any trace amounts of water in the system have the potential to form 1,1,3,3,5,5,7,7-octamethyltetrasiloxane (OMTS), which would not be removed by boiling. Therefore a silica gel column was used to help remove this and other byproducts of the reaction. Since water can react with the SiH group and decrease yield, the column was dried by blowing argon through the column while heating it with a propane torch. The column was then loaded with anhydrous hexane as the solvent. After a solution of toluene/hexane containing the mesogen was added to the column, a generous amount of hexane was run through the column to remove the OMTS. Since the mesogen barely moves down the column with hexane, an anhydrous solution of 33% toluene in hexane was used to remove it from the column and to fractionate out other byproducts.

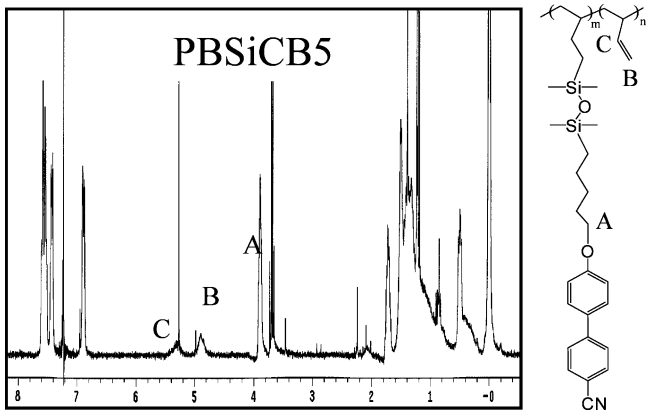

Figure 2. NMR spectrum of PBSICB5 used to calculate the fractional attachment of mesogen to the pendant vinyl groups. The mole fraction of the different monomeric units of mesogen, 1,2-butadiene, and 1,4-butadiene can be calculated from the peak areas A, B, and C as: $f_{\text{mesogen}} = (2A)/(2A + B + 2C)$, $f_{1,2} = (2B)/(2A + B + 2C)$, and $f_{1,4} = (2C - B)/(2A + B + 2C)$, respectively.

Once purified, the functionalized mesogen CBSi5 was attached to the 1,2-polybutadiene backbone by mixing them in an anhydrous solution of THF and toluene with a few drops of the catalyst PCO85. To account for any losses due to purification, the functionalized mesogen was added at 3 times excess based on the amount of CBV5 initially used relative to pendant vinyl groups on the polymer backbone. The excess mesogen also had the effect of pushing the reaction closer to completion in a reasonable amount of time. The reaction was allowed to progress for 3 or 4 days even though 80−90% attachment of the mesogen was typically achieved in 2 days. The reaction was quenched by the addition of an excess of a vinyl-containing compound, such as styrene, to neutralize the reactive end of any disiloxane compounds that may have been partially attached to the polymer backbone. After a day of quenching the reaction, the product polymer was precipitated two−three times by addition of methanol to a solution of the polymer in THF resulting in an overall yield of 90%.

The fractional attachment of the mesogen was determined by NMR (Figure 2) and found to be between 87 and 94%. The polydispersity index (PDI), characterized using gel permeation chromatography in THF solution (Waters 401 differential refractometer with two 30 mm long Polymer Laboratories PLgel 10 mm analytical columns connected in series, calibrated against monodisperse polystyrene standards), was between 1.1 and 1.8. Most of the broadening (the initial 1,2-polybutadienes had a PDI = 1.04) of the molecular weight distribution was apparent after the sample was precipitated out of solution and allowed to stand for a period of a day following the end of the reaction. After several days the polymer exhibited long-term stability with virtually no change in the PDI. It was stored with ∼1% inhibitor, octadecyl 3-(3,5-di-*tert*-butyl-4-hydroxphenyl)propionate. It is presumed that broadening of the molecular weight distribution is a consequence of some polymer−polymer coupling (i.e., cross linking) due to disiloxanes formed from the dihydroxy-biphenyl precursor.

This synthesis protocol gave rise to a polymer, designated PBSiCB5, that was smectic at temperatures below 60 °C and isotropic at temperatures above roughly 70 °C. Further characterization was performed by differential scanning calorimetry (DSC; Perkin-Elmer DSC 7 using Pyris software) and polarizing optical microscopy (POM; Zeiss polarizing microscope with Mettler FP82 hot stage). DSC experiments were first performed by heating the sample well into the isotropic phase to remove any thermal history and then cooling at 10 °C/min to a low temperature. Subsequent heating scans at 10 °C/min reveal the polymers to be glassy, with a glass transition temperature of approximately −10 °C for all samples, and a

Table 1. Physical Property Characterization and Phase Transition Temperatures for SGLCPs Used in This Investigation

M (kg/mol)[a]	M_w/M_n[b]	% substitution[c]	T_i (°C)[d]
91	1.10	91	79.5
434	1.10	91	70.0
518	1.59	94	65.3
690	1.83	87	63.0
1900	1.90	83	64.0

[a] The molecular mass (M) refers to that of the entire side-chain LCP sample, consisting of both the parent polymer and side group, and was calculated based on the fractional substitution of mesogenic groups. [b] Polydispersities were measured using GPC. [c] The percent substitution was determined by NMR by comparing the integrated areas of the peaks due to pendant vinyl groups to peaks associated with the mesogenic groups. [d] The isotropization temperature (T_i) was detected by DSC and measured at the peak of the transition.

clearing temperature that varies somewhat among the different polymers studied. POM during heating (1−5 °C) shows a transition from a birefringent liquid−crystal phase below the DSC-measured transition temperature to an isotropic phase at high temperatures; however, the mesophase defect texture was very fine so that no conclusions could be drawn from POM about the type of liquid−crystal ordering present at lower temperatures (X-ray diffraction results presented below provide positive evidence of smectic ordering). Physical properties and characterization (molecular masses, polydispersities, and DSC-determined clearing temperatures) of the synthesized polymers are summarized in Table 1.

2.2. Rheology. Mechanical characterization was performed using a Rheometrics (RSA II) dynamic mechanical testing system. Oscillatory strain frequencies typically covered a range of four decades (0.01−100 rad/s). Temperature control was achieved by circulating air or nitrogen through the environmental chamber. The uniformity and stability of the temperature were specified to be ±0.5 °C. A "shear sandwich" geometry was used to perform rheological measurements in which a gap thickness between 0.32 and 0.55 mm was used for the different samples. Melt films of excess initial thickness were pressed into the fixtures and subsequently trimmed to the fixture dimensions. To provide a reproducible initial condition, samples were heated at least 10 °C into the isotropic phase and held there for at least 10 min before each set of experiments to erase effects of sample loading or any previous strain history. Strain sweep experiments were used to define the range of linear dynamic response; all frequency sweep data reported in this paper were collected at small strain amplitude (<5%) in the linear regime. The effect of large amplitude oscillatory shear on the structure and rheology of these polymers is described separately.[21]

2.3. X-ray Experiments. A modified Linkam CSS-450 high-temperature shearing stage, described by Ugaz and Burghardt,[29] was used to carry out small-angle X-ray scattering (SAXS) experiments. The shear stage provided a parallel disk shearing geometry with a sample thickness of 1 mm. Thin Kapton sheets glued to both the fixed and the rotating plates served as the X-ray windows. An aperture hole located in the fixed plate defined the size of the incident beam (1 mm diameter). X-ray experiments were performed on beamline 5BM-D of DND-CAT at the Advanced Photon Source of Argonne National Laboratory. The highly collimated X-ray beam had an energy of 25 keV (λ = 0.496 Å). The use of relatively high energy confined scattering to smaller angles allowing both wide- and small-angle scattering to more easily exit the shear cell. Digital two-dimensional scattering patterns were collected using a charge-coupled device detector (MarCCD). Since a rotating disk geometry was used, scattering patterns reflect flow-induced variations in molecular orientation within the plane defined by the flow and vorticity directions (1,3-plane). Here we only present data collected under quiescent conditions on previously aligned specimens.

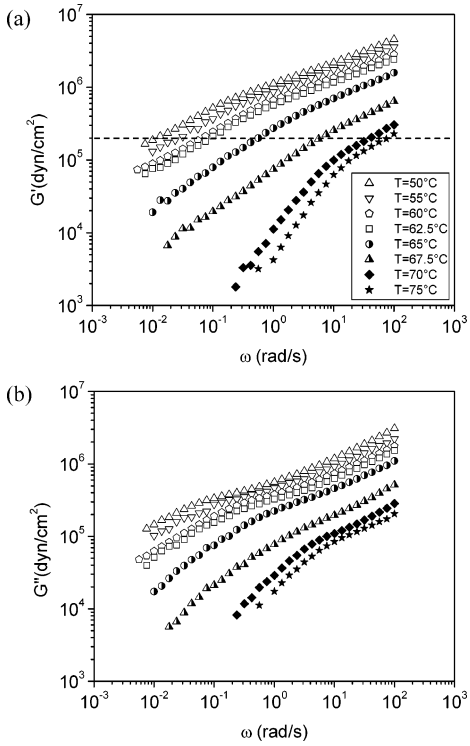

Figure 3. Unshifted (a) storage modulus and (b) loss modulus data for 518 kg/mol PBSiCB5 at indicated temperatures.

3. Results and Discussion

3.1. Linear Viscoelastic Response and Phase Behavior of 518 kg/mol PBSiCB5. The storage and loss moduli, G' and G'', (parts a and b of Figure 3, respectively) of the SGLCPs were measured at temperatures ranging from 30 to 80 °C. At the highest temperatures ($T \geq 70$ °C for the 518 kg/mol sample of Figure 3) G' and G'' tend toward conventional terminal relaxation ($G' \approx \omega^2$ and $G'' \approx \omega$) at low frequencies and Rouselike behavior (G', $G'' \approx \omega^{1/2}$) at high frequencies. The failure to perfectly achieve the limiting terminal slopes may be related to force limitations in these low-frequency measurements. Within this high-temperature regime, identified as the isotropic phase using polarized optical microscopy, the relaxation time decreases with increasing temperature, while the shapes of the curves do not change. At somewhat lower temperatures ($62.5 < T < 70$ °C), the complex modulus changes rapidly, indicating both a dramatic slowing down of the dynamics and a change of shape in the G' and G'' curves, which no longer show terminal behavior. Finally, at low temperatures ($T \leq 62.5$ °C) the temperature dependence decreases and the G' and G'' curves again adopt self-similar (but nonterminal) shapes. The general trends in Figure 3 resemble unshifted linear viscoelastic data reported by Lee and Han for other smectic SGLCPs.[20] Such dramatic changes in the linear viscoelastic response are a common signature of ordering transitions.

X-ray scattering was used to elucidate the structural origins of the transition region between 62.5 and 70 °C in 518 kg/mol PBSiCB5 (Figure 4). At a temperature of 60 °C, X-ray scattering showed the sample to be smectic, with a sharp layer reflection peak at low angles ($q^* = 0.234$ Å^{-1}) corresponding to a d spacing of 27 Å indicating that the side groups are highly interdigitated. When quenched from the isotropic phase at high temperatures, there is no macroscopic orientation, and 2-D scattering patterns are isotropic. However, large amplitude oscil-

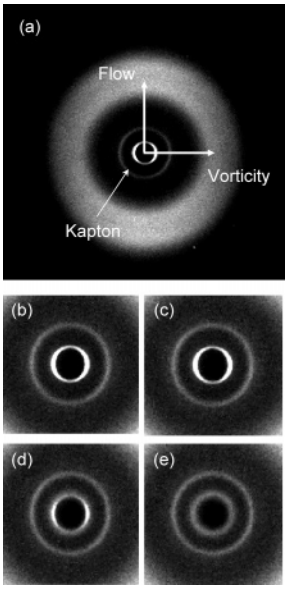

Figure 4. X-ray scattering patterns for 518 kg/mol PBSiCB5. (a) Quiescent 2-D pattern in the smectic phase (60 °C) after sample had been sheared at 0.05 Hz and 95% strain for 62 min, followed by relaxation for 12 min. The isotropic ring at intermediate q arises from the Kapton windows in the shear cell. Also shown are quiescent images expanded to emphasize changes in smectic reflection during heating at 61 (b), 65 (c), 69 (d), and 73 °C (e).

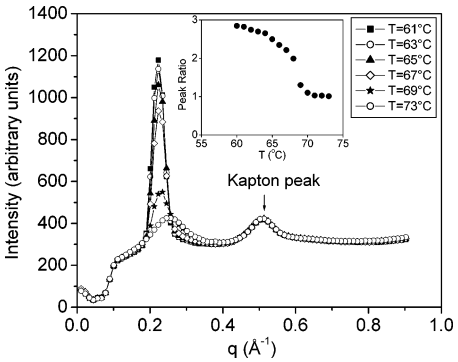

Figure 5. Azimuthally averaged X-ray scattered intensity, $I(q)$, for 518 kg/mol PBSiCB5 at different temperatures. Insert shows ratio of intensity of smectic to Kapton peak as a function of temperature.

latory shear is capable of inducing macroscopic alignment in the sample (Figure 4a). The low q diffraction from smectic layers is concentrated along the vorticity direction, indicating that shear promotes orientation in the "perpendicular" state, where layers lie within the flow-gradient plane. The diffuse wide-angle mesogen peak at higher q is also rendered anisotropic by shear, with intensity concentrated perpendicular to the smectic reflections, indicating ordering of the smectic-A type.

The anisotropic, shear-aligned PBSiCB5 sample was quiescently heated in 1 °C increments through the range of temperatures (60−80 °C) where the dramatic changes in rheology are observed. Upon heating from the smectic state, a broad smectic−isotropic transition is manifested by the gradual reduction in intensity and broadening of the low q smectic reflection (parts b−e of Figure 4). Azimuthally averaged $I(q)$ scans in the small-angle regime show a systematic drop in smectic peak intensity with increasing temperature (Figure 5). To quantify these changes, we take the ratio of the smectic peak height to that of the peak arising from the Kapton shear

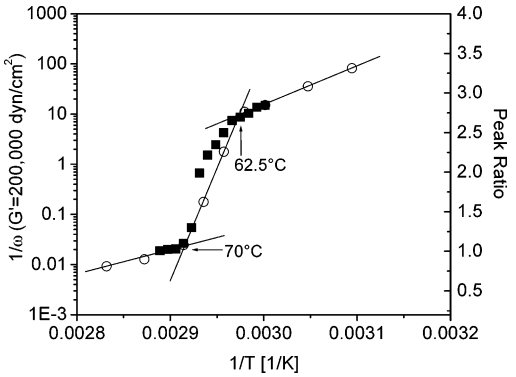

Figure 6. Effect of temperature on dynamics of 518 kg/mol PBSiCB5. One over the angular frequency at which $G' =$ 200 000 dyn/cm^2 (see dashed line in Figure 3a) is plotted as a function of inverse temperature (circles). An overlay compares these results with the X-ray peak intensity ratio data from Figure 5 (squares).

cell windows, which provides a convenient internal standard (Figure 5 insert). This quantifies the gradual loss of the smectic phase and demonstrates that the rapid change in dynamics in the temperature range of 62.5−70 °C is associated with a broad smectic−isotropic biphasic region.

A simple quantitative analysis of the rheological data allows determination of the width of the biphase region. We take one over the angular frequency at which $G' =$ 200 000 dyn/cm^2 as a convenient indicator of the changes in time scale with frequency over the temperature range of interest (an arbitrary choice of condition, but one which is encompassed by most of the data sets in Figure 3). These results show that the temperature dependence clearly breaks into three regions and, further, that the intermediate regime of rapid change is well correlated with the X-ray results indicating a smectic−isotropic biphase (Figure 6). Intersections between lines fit to data in each regime allows accurate rheological determination of the location and width of the biphasic regime. A similar procedure was used for samples of varying molecular weight; in all samples studied using both rheology and X-ray scattering, good agreement was found with these independent measures of the location and width of the biphasic regime (Table 2). We attribute the biphasic region to heterogeneity in the degree of substitution of the mesogenic side chains. This is discussed further in section 3.3 below.

3.2. Temperature Dependence of Dynamics in 518 kg/mol PBSiCB5. A Cole−Cole plot (G' vs G'', Figure 7) demonstrates thermo-rheological complexity as this material passes through its ordering transition; the failure of data to superimpose indicates differences in the shape of the relaxation spectrum in the various temperature regimes. At the same time, data collected *within* either the smectic or isotropic phases do separately collapse in the Cole−Cole representation, indicating temperature independence in the shape of the relaxation spectrum. This provides justification for using time−temperature shifting to explore the temperature dependence of dynamics in either phase. While the ability to shift data within the isotropic phase is not surprising, there are many reasons to expect that this might not be possible within the smectic phase. Temperature-dependent changes in the thermodynamic state of the SGLCP (e.g., order parameter) or contributions of distortional elasticity to the measured moduli are two examples of phenomena that could lead to more

Table 2. Phase Transition Temperatures Determined through Rheology and X−ray Scattering Experiments

M (kg/mol)	$T_{s-biph.}$ (°C)[a]	$T_{biph.-i}$ (°C)[a]	ΔT_{i-s} (°C)	$T_{s-biph.}$ (°C)[b]	$T_{biph.-i}$ (°C)[b]	ΔT_{i-s} (°C)
91		82.5				
434	55.0	75.0	20		75.0	
518	62.5	70.0	7.5	62.0	70.0	8
690	61.0	65.0	4	63.0	65.0	2
1900	61.0	63.5	2	62.0	63.0	1

[a] Phase transition temperatures determined rheologically. [b] Transition temperatures determined by X-ray scattering.

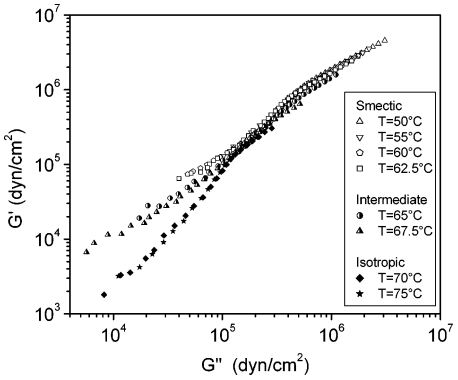

Figure 7. Cole−Cole plot of the storage modulus vs the loss modulus for 518 kg/mol PBSiCB5 at different temperatures.

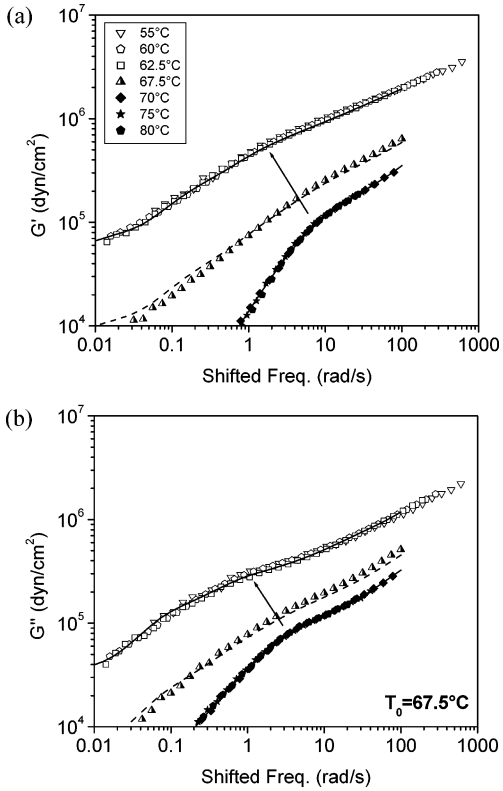

Figure 8. (a) Storage and (b) loss modulus of 518 kg/mol PBSiCB5, in which smectic and isotropic data have been *separately* time−temperature superimposed and then shifted to 67.5 °C (a temperature in the biphasic region) by small extrapolations using the activation energies measured in each phase. Solid curves represent generalized Maxwell fits to the smectic and isotropic data, while the heavy dashed curve represents prediction of a linear mixing rule, eq 1, using $x = 0.13$. Arrows represent a possible interpretation of the rheological changes accompanying the isotropic−smectic transition; see discussion in text.

complex temperature-dependent changes in the relaxation spectrum. Despite these potential complications, the data themselves testify that superposition is possible in this case. Indeed, previous literature results have generally demonstrated the ability to construct master curves within smectic phases via time−temperature shifting,[6,13,19] and this procedure has been widely adopted.

Data collected in the smectic ($T \leq 62.5$ °C) and isotropic ($T \geq 70$ °C) phases were first shifted to create separate master curves. Over the temperature ranges studied, the temperature dependence could be described by an Arrhenius expression with activation energies of 45 and 61.5 kJ/mol, respectively, for the isotropic and smectic phases. To clarify the nature of the rheological changes associated with the phase change itself, these master curves were shifted to a common temperature of 67.5 °C, within the biphasic region, via small extrapolations using the activation energies measured within either phase (Figure 8). This procedure is similar to that adopted by Colby et al. in which separate master curves from smectic and nematic phases of a SGLCP were shifted to a common reference temperature.[6] As in that case, this representation reinforces the dramatic qualitative and quantitative changes to the dynamics associated with smectic ordering (although here, of course, it is the smectic and isotropic phases that are being compared). Data collected within the biphasic region at $T = 67.5$ °C are surprisingly well represented by a simple linear mixing rule

$$\bar{G}^* = xG_i^* + (1 - x)G_s^* \quad (1)$$

which interpolates between the smectic and isotropic results as x increases from 0 to 1. (Predictions of eq 1 in Figure 8 were generated by first fitting the smectic and isotropic relaxation moduli to a generalized Maxwell spectrum and then using these analytical expressions to compute $\bar{G}^*$.) From Figure 3, it is clear that decreasing temperature within the biphase leads to rheology closer to that found in the smectic phase, as a larger fraction of the polymer undergoes ordering.

The changes in G' and G'' upon ordering may be attributed to an increase in modulus due to the additional ordered fluid structure or, alternatively, to a slowing down of the chain dynamics caused by the topological restrictions imposed by localization of mesogens in smectic layers. The latter viewpoint has been frequently adopted in the literature. Drawing upon procedures originally developed in the context of microphase separation in lamellar block copolymers,[30] Rubin and co-workers[13] used time−temperature shifting to collapse data collected in the isotropic, nematic, and smectic phases of different SGLCP polymers in the limit of high frequency, hypothesizing that the shape of the relaxation spectrum at high frequencies (i.e., local chain dynamics) will be unaffected by ordering at larger length scales. Similar procedures have subsequently been adopted by other investigators,[19] although the use of *any* time−temperature shifting procedures in ordered polymers has also received criticism.[20] Partial support for this approach in the present case comes from the near superposition of the high-frequency isotropic data with the smectic data in the Cole−Cole plot (Figure 7).

Results of a shifting procedure which attempts superposition of all data at high frequency are presented in Supporting Information available for this paper. These results allow comparison to other literature reports in which this procedure has been used,[13,19] but we do not believe the procedure is warranted in this case. First and foremost, it is not obvious that concepts applied successfully to lamellar block copolymers should necessarily translate to SGLCPs. In the former case, the ordered layers possess a length scale comparable to the radius of gyration of the full chain, so that a reasonable separation of time scales for layer dynamics and the Rouselike dynamics of subchains may be expected. For entangled hydrocarbon block copolymers of higher molecular weight, the entanglement length provides an additional intermediate length scale whose dynamics are still observable within the ordered lamellar phase.[30] Conversely, the ordered layers in smectic SGLCPs adopt the length scale of the mesogens and hence the monomers themselves. Under conditions in which a single statistical segment of the chain in the isotropic melt may possibly participate in multiple smectic layers upon ordering, it is difficult to imagine that *any* length scale is sufficiently "local" (except perhaps at the very high frequencies of the dynamic glass transition) to render high-frequency chain dynamics in the isotropic and smectic phases similar enough to rationalize this type of shifting.

The coincidence of smectic and isotropic data in a Cole−Cole plot such as Figure 7 may, indeed, be mere coincidence. As in the case of the 518 kg/mol PBSiCB5 polymer highlighted here, such collapse of the data often involves high-frequency isotropic data in which Rouselike behavior, G', $G'' \approx \omega^{1/2}$, is observed (as befits the notion of local chain motion). However, ordered fluids with layered morphologies frequently also exhibit the same power-law scaling.[18,30] By the Kramers−Kronig relations, power-law rheology with an exponent of $^1/_2$ must also be characterized by $G' = G''$. In other words, Rouselike and typical layerlike rheological behavior must fall along a common line on a Cole−Cole plot. Superposition of the type seen in Figure 7 does not necessarily signify similarity of mechanism at the molecular or mesoscopic level.

Attempts to create master curves in these smectic SGLCPs by superposing "high" frequency data are also limited by the narrow range of overlap between data sets, itself a consequence of the dramatic rheological changes observed upon ordering (Figure 3). In the earlier work of Rubin and co-workers, the dynamic differences between the isotropic, nematic, and smectic phases were less dramatic than those found here, leading to a wider range of overlap in the master curves obtained by this procedure. Certainly, the superposition of isotropic and nematic data by Rubin and co-workers seems robust given the wide range of frequency overlap available and the high quality of the superposition achieved at high frequencies;[13] also note that Colby et al. successfully superimposed data from isotropic and nematic phases.[6] In this vein, it is interesting to note that Lee and Han observed a nearly perfect superposition of data for isotropic and nematic phases in a $G'-G''$ plot for a nematic SGLCP, from which they conclude that the dynamic consequences of the isotropic−nematic transition are not as severe as for the isotropic−smectic transition,[20] a conclusion consistent with earlier observations of nematic SGLCP rheology.[6−8] (Recall that Rubin and co-workers *did* see clear rheological consequences of nematic ordering at low frequency[13] but were using very high molecular weight polymers relative to that studied by Lee and Han.)

In the absence of isotropic phase data at much higher frequencies (a difficult proposition for routine methods of melt rheometry), we favor the representation of Figure 8 for the SGLCPs considered here. This presentation highlights the rheological consequences of mesophase formation without imposing an implicit assumption that these rheological changes only reflect a slowing down of dynamics (i.e., a horizontal shift). While it is probably impossible to decompose these changes with certainty, it is reasonable to postulate smectic ordering of SGLCPs might be accompanied by both a slowing down of dynamics and an additional contribution to the modulus, which would move the curves vertically. In the case of the PBSiCB5 sample in Figure 8, it is interesting to note that the smectic phase data are not a featureless power law but show signs of a relaxation process at intermediate frequencies. If one postulates that this is related to the overall chain dynamics (which we recognize to be a speculative assumption), comparison with the chain relaxation in the isotropic data suggests that smectic ordering leads to both dynamic slowing (horizontal shift) as well as modulus enhancement (vertical shift), as represented by the arrows in Figure 8. This notion is similar in spirit to the observations of Colby et al. that enhanced elastic character in a smectic SGLCP extends to much lower frequencies than estimates of the time scale for overall chain motion from diffusion measurements, suggesting that it is associated with structural elements much larger than the typical coil size (e.g., smectic grain structures).[6]

3.3. Effect of Fractional Mesogenic Substitution and Molecular Weight on the Biphasic Regime. A series of polymers having the same mesogenic structure but differing in their molecular weight were made in order to determine the effect on polymer rheology and phase behavior. As shown in Table 2, all the samples had a biphasic region between the isotropic and smectic phases. Maintaining low polydispersity while achieving a high degree of attachment of mesogenic groups was difficult at larger molecular weights; therefore, an increase in molecular weight was accompanied by an increase in polydispersity and a decrease in the degree of attachment. Tables 1 and 2 demonstrate that higher molecular samples generally showed lower transition temperatures and narrower biphasic windows. Which molecular parameters control the temperature and width of the smectic−isotropic transition? Wewerka et al. found that a higher degree of polymerization of the polymer backbone increased isotropic-to-mesophase transition temperatures in their side-chain polymers,[19] while the opposite trend is observed here. Their work considered molecular weights that were much lower than those of our samples, such that chain-end effects could play a significant role. Since a chain end is likely to be a source of local disruption in the liquid-crystalline order, a greater fraction of chain ends leads to a greater perturbation to the LC structure and hence to a lower clearing temperature. Conversely, our study employed very large molecular weight samples, where effects of chain ends on transition temperatures should be negligible. Under these conditions, molecular weight polydispersity is also not expected to lead to significant broadening of the transition; for instance, Kasko et al.[31]

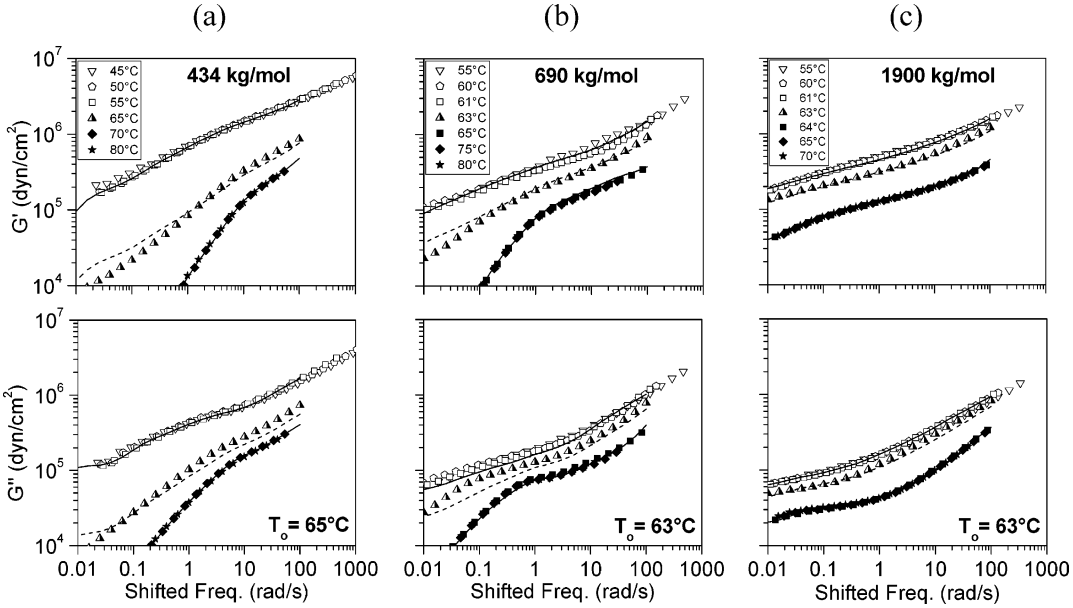

Figure 9. Effect of PBSiCB5 molecular weight on the linear viscoelastic response. Rheological master curves for (a) 434, (b) 690, and (c) 1900 kg/mol PBSiCB5 samples were prepared using the procedures of Figure 7, in which separate smectic and isotropic phase master curves were prepared and shifted to a common reference temperature in the biphase region for each sample. Dashed curves represent the prediction of a linear mixing rule, eq 1, using (a) $x = 0.12$, (b) $x = 0.40$, and (c) $x = 0.56$.

found that polymers having a broad Gaussian-like distribution of chain lengths (i.e., broader PDI) did not exhibit broadening of the T_{s-i} region. Instead, the changes in $T_{biph.-i}$ and ΔT_{i-s} observed here are most likely the result of changes in the degree of mesogenic substitution rather than the DP or polydispersity.

Similar to the role of chain ends in lower molecular weight samples, monomeric units without mesogens would be expected to disrupt molecular packing and consequently lower the transition temperature. Any branches associated with sparse cross linking in the higher molecular weight samples (the presumed origin of the higher polydispersity) would also serve to disrupt molecular packing and suppress T_{s-i}; however, given the reduced degree of mesogen substitution found at high molecular weights (Table 1), "missing mesogen defects" should be much more prevalent than branch points and are thus likely the primary factor explaining the trend toward lower clearing points. The consequences of random and incomplete mesogen attachment can be considered in relation to concepts of Stupp et al.,[32] who discuss the origins of a biphasic region in a melt of a main chain nematic random copolymer of monomers of different intrinsic stiffness. They invoke the concept of "polyflexibility," referring to a distribution of chain flexibility, reflecting in turn the statistical distribution of composition among individual molecules in a random copolymer. This varying degree of flexibility will cause the stiffer molecules to transition at lower temperatures than more flexible molecules, leading to a biphasic region. This reasoning transfers to our systems in that incomplete mesogen attachment renders our SGLCPs random copolymers. Individual molecules within the sample will thus exhibit a statistical distribution of degree of mesogen attachment, allowing a biphasic region in which molecules with higher mesogen content are preferentially partitioned into the smectic phase.

These concepts may be extended to rationalize why the width of the biphasic region decreases in samples of larger molecular weight (Table 2). As DP increases, it is statistically more likely that each molecule in a random copolymer will approach the mean composition of the sample as a whole. This reduction in the compositional heterogeneity of the sample would result in a corresponding decrease in the width of the two-phase region. Detailed testing of these hypotheses would require further experiments on samples with varying molecular weights but the same degree of substitution (and vice versa), which presents a significant challenge in synthesis and characterization.

3.4. Effect of Molecular Weight on Rheology. Smectic ordering leads to similar rheological consequences for all molecular weights of PBSiCB5 studied (Figure 9). Comparison of isotropic and smectic data shifted to a common temperature in the biphase reveals evidence of retarded dynamics and/or moduli enhancement for all molecular weights studied. In each case, the simple linear mixing rule (eq 1) can provide a reasonable representation of data collected in the biphase region. Note that because of the sample-dependent location and width of the biphase, and the particular temperatures chosen for rheological study, these plots differ slightly in the choice of reference temperature within the biphase regime.

As expected, the isotropic phase data show a strong dependence on molecular weight and, in particular, demonstrate the emergence of an entanglement plateau for the higher molecular weight samples. The plateau modulus is estimated as the value of G' where the phase angle is at its minimum,[33] leading to $G_N^0 \approx 1.15 \times 10^5$ dyn/cm^2, quite similar to that found in the SGLCP studied by Rubin and co-workers (1.2×10^5 dyn/cm^2).[13] Conversely, there is only a weak effect of molecular weight on the rheology within the smectic phase, consistent with the hypothesis that the smectic rheology is dominated by layer dynamics, in which polymer molecular weight does not play a significant role. There do appear to be small qualitative changes in the low frequency portion of the smectic response as molecular weight increases and entanglement dynamics emerge.

Higher molecular weights (in which the plateau extends to lower frequencies) would presumably lead to more dramatic changes in the low-frequency smectic response.

4. Conclusions

We have synthesized new model 1,2-polybutadiene-based thermotropic SGLCPs with cyano-biphenyl mesogenic side groups with relatively low polydispersity and high molecular weight. Rheology and X-ray methods were used to characterize their phase structure and viscoelastic properties and showed that these polymers exhibit smectic ordering in the liquid crystalline state. The linear viscoelastic behavior is strongly affected by the smectic ordering. The temperature dependence of the dynamics reveals the existence of three distinct regimes, which X-ray scattering demonstrated to be smectic at low temperatures (T < 60 °C), isotropic at high temperatures (T > 80 °C), and an intermediate smectic−isotropic biphase. The presence of this biphasic region is attributed to the incomplete attachment of the mesogenic units to the pendant vinyl groups of the 1,2-polybutadiene pre-polymer and the resulting statistical distribution of composition within the polymer sample. This concept allows rationalization of how the location and width of the biphase region varies with polymer composition and molecular weight. While smectic SGLCP data have frequently been shifted to create master plots in which isotropic and smectic data are superimposed in the high-frequency limit,[13,19] we question whether such a representation can be justified in the present case. We suggest an alternate representation of the data that emphasizes rheological consequences of ordering while requiring fewer assumptions. The isotropic phase rheology is strongly dependent on molecular weight and shows the emergence of an entanglement plateau for high molecular weight samples. Conversely, the smectic phase rheology does not depend as strongly on polymer molecular weight, consistent with the assumption that the viscoelastic response is dominated by the smectic layers.

Acknowledgment. We gratefully acknowledge financial support from the Air Force Office of Scientific Research (AFOSR)-LC MURI (f4962-97-1-0014), Fundación Antorchas (Argentina), CONICET (Argentina), and the National Science Foundation (DMI-0132519). X-ray scattering experiments were conducted at the DuPont−Northwestern−Dow Collaborative Access Team (DND-CAT) Synchrotron Research Center located at Sector 5 of the Advanced Photon Source of Argonne National Laboratory. DND-CAT is supported by the E.I. DuPont de Nemours & Co., the Dow Chemical Company, and the National Science Foundation through Grant DMR-9304725 and the State of Illinois through the Department of Commerce and the Board of Higher Education Grant IBHE HECA NWU 96. Use of the Advanced Photon Source was supported by the U.S. Department of Energy, Basic Energy Sciences, Office of Energy Research, under Contract No. W-31-102-Eng-38.

Supporting Information Available: Text discussing a shifting procedure within a single master plot and figures showing storage modulus and loss modulus master curves for 518 kg/mol PBSiCB5 and time−temperature shift factors obtained from shifting the data from Figure 8. This material is available free of charge via the Internet at http://pubs.acs.org.

References and Notes

(1) Hsu, C. S. *Prog. Polym. Sci.* **1997**, *22*, 829.
(2) Shibaev, V. P.; Kostromin, S. G.; Plate, N. A.; Ivanov, S. A.; Vetrov, V. Y.; Yakovlev, I. A. *Polym. Commun.* **1983**, *24*, 364.
(3) Eich, M.; Wendorff, J. H.; Ringsdorf, H.; Schmidt, H. W. *Makromol. Chem.* **1985**, *186*, 2639.
(4) Cabrera, I.; Krongauz, V. *Macromolecules* **1987**, *20*, 2713.
(5) Cabrera, I.; Krongauz, V.; Ringsdorf, H. *Angew. Chem., Int. Ed.* **1987**, *26*, 1178.
(6) Colby, R. H.; Gillmor, J. R.; Galli, G.; Laus, M.; Ober, C. K.; Hall, E. *Liq. Cryst.* **1993**, *13*, 233.
(7) Kresse, H.; Stettin, H.; Tennstedt, E.; Kostromin, S. *Mol. Cryst. Liq. Cryst.* **1990**, *191*, 135.
(8) Findlay, R. B. *Mol. Cryst. Liq. Cryst.* **1993**, *231*, 137.
(9) Porter, R. S.; Johnson, J. F. In *Rheology*; Eirich, F. R., Ed.; Academic Press: New York, 1967; Vol. 4, Chapter 5.
(10) Wissbrun, K. F.; Griffin, A. C. *J. Polym. Sci. Pol. Phys.* **1982**, *20*, 1835.
(11) Baird, D. G. In *Liquid Crystalline Order in Polymers*; Blumstein, A. Y., Ed.; Academic Press: New York, 1978.
(12) Papkov, S. P.; Kulichik, Vg; Kalmykov, Vd; Malkin, A. Y. *J. Polym. Sci. Pol. Phys.* **1974**, *12*, 1753.
(13) Rubin, S. F.; Kannan, R. M.; Kornfield, J. A.; Boeffel, C. *Macromolecules* **1995**, *28*, 3521.
(14) Berghausen, J.; Fuchs, J.; Richtering, W. *Macromolecules* **1997**, *30*, 7574.
(15) Fourmaux-Demange, V.; Brulet, A.; Cotton, J. P.; Hilliou, L.; Martinoty, P.; Keller, P.; Boué, F. *Macromolecules* **1998**, *31*, 7445.
(16) Quijada-Garrido, I.; Siebert, H.; Friedrich, C.; Schmidt, C. *Macromolecules* **2000**, *33*, 3844.
(17) Lee, K. M.; Han, C. D. *Macromolecules* **2002**, *35*, 6263.
(18) Larson, R. G.; Winey, K. I.; Patel, S. S.; Watanabe, H.; Bruinsma, R. *Rheol. Acta* **1993**, *32*, 245.
(19) Wewerka, A.; Viertler, K.; Vlassopoulos, D.; Stelzer, F. *Rheol. Acta* **2001**, *40*, 416.
(20) Lee, K. M.; Han, C. D. *Macromolecules* **2003**, *36*, 8796.
(21) Rendon, S.; Burghardt, W. R.; Auad, M. L.; Kornfield, J. A., in preparation.
(22) Halasa, A. F.; Lohr, D. F.; Hall, J. E. *J. Polym. Sci., Part A: Polym. Chem.* **1981**, *19*, 1357.
(23) Bywater, S.; MacKerron, D. H.; Worsfold, D. J.; Schue, F. *J. Polym. Sci., Polym. Chem. Ed.* **1985**, *23*, 1997.
(24) Sanger, J.; Tefehne, C.; Lay, R.; Gronski, W. *Polym. Bull.* **1996**, *36*, 19.
(25) Hempenius, M. A.; Lammertink, R. G. H.; Vancso, G. J. *Macromol. Rapid Commun.* **1996**, *17*, 299.
(26) Hempenius, M. A.; Lammertink, R. G. H.; Vancso, G. J. *Macromolecules* **1997**, *30*, 266.
(27) Moment, A.; Miranda, R.; Hammond, P. T. *Macromol. Rapid Commun.* **1998**, *19*, 573.
(28) Moment, A.; Hammond, P. T. *Polymer* **2001**, *42*, 6945.
(29) Ugaz, V. M.; Burghardt, W. R. *Macromolecules* **1998**, *31*, 8474.
(30) Rosedale, J. H.; Bates, F. S. *Macromolecules* **1990**, *23*, 2329.
(31) Kasko, A. M.; Grunwald, S. R.; Pugh, C. *Macromolecules* **2002**, *35*, 5466.
(32) Stupp, S. I.; Wu, J. L.; Moore, J. S.; Martin, P. G. *Macromolecules* **1991**, *24*, 6399.
(33) Wu, S. *J. Polym. Sci., Polym. Phys. Ed.* **1987**, *25*, 2511.

MA050551F